Power dissipation in nanoscale conductors

2002 J. Phys.: Condens. Matter 14 5377

(http://iopscience.iop.org/0953-8984/14/21/312)

INSTITUTE OF PHYSICS PUBLISHING JOURNAL OF PHYSICS: CONDENSED MATTER

J. Phys.: Condens. Matter **14** (2002) 5377–5389 PII: S0953-8984(02)34154-7

Power dissipation in nanoscale conductors

M J Montgomery[1], **T N Todorov**[1] **and A P Sutton**[2]

[1] School of Mathematics and Physics, Queen's University of Belfast, Belfast BT7 1NN, UK
[2] Department of Materials, University of Oxford, Parks Road, Oxford OX1 3PH, UK

Received 22 February 2002, in final form 17 April 2002
Published 16 May 2002
Online at stacks.iop.org/JPhysCM/14/5377

Abstract

A previous tight-binding model of power dissipation in a nanoscale conductor under an applied bias is extended to take account of the local atomic topology and the local electronic structure. The method is used to calculate the power dissipated at every atom in model nanoconductor geometries: a nanoscale constriction, a one-dimensional atomic chain between two electrodes with a resonant double barrier, and an irregular nanowire with sharp corners. The local power is compared with the local current density and the local density of states. A simple relation is found between the local power and the current density in quasiballistic geometries. A large enhancement in the power at special atoms is found in cases of resonant and anti-resonant transmission. Such systems may be expected to be particularly unstable against current-induced modifications.

1. Introduction

In recent years it has become possible experimentally to produce a wide variety of conducting nanoscale junctions. Examples of such systems are metallic nanowires and molecular junctions between macroscopic electrodes. The local electrical current densities in such nanojunctions can exceed by many orders of magnitude those in ordinary macroscopic metals. As a consequence of this, electrical current flow can affect significantly the structure and mechanical properties of a nanojunction. Progress has been made in the modelling of current-induced forces in these systems [1–9]. It has been shown that current-induced changes to interatomic bond forces can result in a dramatic reduction in the strength and stability of atomic wires [5]. However, a full understanding of current-induced mechanical effects is not possible without knowledge of the effective local temperature in a nanoscale conductor in the presence of current flow [5].

The origin of current-induced local heating in nanoscale conductors is fundamentally the same as in ordinary macroscopic metals. The current-carrying electrons are effectively in an excited state and are able to dissipate heat by losing energy to phonons via non-adiabatic, inelastic electron–phonon collisions. The difference between heating in atomic-scale conductors and heating in ordinary bulk conductors is threefold. First, the characteristic energy scales involved are different. Atomic-scale conductors often operate in the limit $|eW| \gg k\theta$, $|eW| \gg \hbar\omega$, where W is the applied voltage across the electrodes, θ is the ambient temperature,

0953-8984/02/215377+13$30.00

and ω is a typical atomic vibration angular frequency. This is the limit that we consider in this paper. This regime may be contrasted with classical diffusive bulk conduction, where the potential drop per electron mean free path is typically much smaller in magnitude than $k\theta/e$.

Second, a nanoscale junction is an inhomogeneous system, in which every atom may have a unique environment. All atoms must be treated explicitly, and on an equal footing, in the modelling of electrical conduction in such systems. Building on past work on current-induced heating of isolated defects [10–12], it has been argued that all atoms in a nanojunction have oscillator degrees of freedom and can exchange energy with the current-carrying electrons [13]. Power dissipation at all atoms must be included in a calculation of local heating [13].

Third, the linear dimensions of a nanojunction are typically much smaller than the inelastic electron mean free path. In other words, the time spent by an electron in the nanojunction is much smaller than the average time between inelastic electron–phonon collisions. Under these conditions, on average each electron that crosses the junction dissipates only a small fraction of its energy in the junction itself. Hence, most of the total power in the circuit is dissipated in the macroscopic electrodes adjoining the junction [13, 14]. However, we may put the question differently and ask not where most of the total power goes, but in what part of the system the highest power dissipation per atom is to be found. This will be in the region where the current density is highest, namely in the nanojunction itself. Notionally, this large power per atom in the nanojunction may be thought of as a product of two factors: the fraction of their energies that electrons dissipate on average while crossing the nanojunction, which is small, and the number density of current-carrying electrons in the nanojunction, as quantified by the local current density, which can be huge.

A simple tight-binding model of electron–phonon coupling suggests that at current densities attainable in metallic nanojunctions, the power per atom in the nanojunction can be sufficiently high to lead to a significant local temperature rise [5, 13]. Experimental evidence for such heating comes from measurements [15–17] of the voltage dependence of

(a) two-level conductance fluctuations and
(b) hystereses at conductance steps in atomic-scale metallic contacts.

Another phenomenon that has been associated with local heating is atom transfer in the scanning tunnelling microscope [18, 19].

The calculations in [13] were based on crude approximations, in which every atom was treated as if it were embedded in a bulk environment. In this paper, we present a tight-binding formalism to calculate the power dissipated at each atom in a general nanojunction geometry, while taking explicit account of the local atomic configurations and the corresponding local electronic structure. We have used this formalism to study the relationship between power dissipation and the local electronic structure and current density in model two-dimensional systems. In the limit where $|eW| \gg k\theta$, $|eW| \gg \hbar\omega$, in quasiballistic geometries, we have found, to a good approximation, that the local power is proportional to the local current density. This simple relationship disappears with increasing scattering. In the cases of resonant and anti-resonant transmission, we have found a great enhancement in the power at special atoms. This suggests that such nanostructures would be particularly prone to current-induced modifications.

2. Method

The general setup that we consider is shown in figure 1. Our system consists of two semi-infinite macroscopic electrodes, connected by a nanoscale junction of arbitrary structure [3, 9, 20–22].

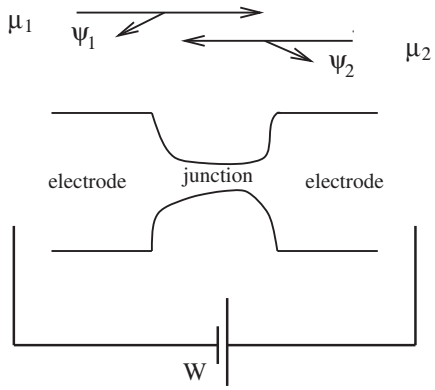

Figure 1. The general setup considered in the paper. The details are discussed in the text.

A voltage W is applied across the electrodes. We calculate the power dissipated into each atom in the junction by perturbation theory, following the framework of [13].

To define the unperturbed state of the electron subsystem, we imagine that the ions are frozen at their equilibrium positions. The electronic structure of the system is described by a single-orbital orthogonal tight-binding model [3, 7, 9, 20–24] with Hamiltonian

$$H_{\mathrm{e}} = \sum_{m,n} |m\rangle H_{mn} \langle n| \tag{1}$$

where $|n\rangle$ is a spherically symmetric positional basis state at atomic site n. The electron eigenstates for the electrode–junction–electrode system can be divided into two classes [3, 9, 20, 22]. The states in one class, $\{|\psi_1\rangle\}$ with energies $\{E_1\}$, consist of a right-travelling wave, incident in the left electrode upon the junction, then partially reflected back into the left electrode and partially transmitted into the right electrode, and conversely for the other class, $\{|\psi_2\rangle\}$ with energies $\{E_2\}$. The battery populates the states $\{|\psi_1\rangle\}$ and $\{|\psi_2\rangle\}$ with Fermi–Dirac occupation functions $f_1(E)$ and $f_2(E) = f_1(E + eW)$, with electrochemical potentials μ_1 and $\mu_2 = \mu_1 - eW$, respectively. Positive eW corresponds to electron flow from left to right. The temperature entering f_1 and f_2 is the ambient temperature θ. The on-site energies $\{H_{nn}\}$, and the states $\{|\psi_1\rangle\}$ and $\{|\psi_2\rangle\}$, may, in general, be calculated in a self-consistent manner, making them implicit functions of the bias W [3, 9]. The intersite Hamiltonian matrix elements $H_{mn} = H_{nm}$ are functions of the interatomic distance and are parameters of the model [3, 7, 9, 23]. The electronic structure of the current-carrying electrode–junction–electrode system in the absence of electron–phonon interactions is thus described by the density operator

$$\rho(W) = \int f_1(E) D_1(E)\, \mathrm{d}E + \int f_2(E) D_2(E)\, \mathrm{d}E \tag{2}$$

where $D_1(E) = \sum_1 |\psi_1\rangle \delta(E - E_1) \langle\psi_1|$ and $D_2(E) = \sum_2 |\psi_2\rangle \delta(E - E_2) \langle\psi_2|$ are the partial density of states operators associated with the two classes of electron states. Rather than calculating the states $\{|\psi_1\rangle\}$ and $\{|\psi_2\rangle\}$ explicitly, one may use scattering theory [20] to express $D_1(E)$ and $D_2(E)$, and the total density of states operator $D(E) = D_1(E) + D_2(E)$, directly in terms of the Green function for the electrode–junction–electrode system as follows [9, 22]

$$2\pi \mathrm{i} D_1(E) = P_1 G^-(E) - G^+(E) P_1 + G^+(E)(P_2 H_{\mathrm{e}} P_1 - P_1 H_{\mathrm{e}} P_2) G^-(E) \tag{3}$$

$$2\pi \mathrm{i} D_2(E) = P_2 G^-(E) - G^+(E) P_2 + G^+(E)(P_1 H_{\mathrm{e}} P_2 - P_2 H_{\mathrm{e}} P_1) G^-(E) \tag{4}$$

$$2\pi \mathrm{i} D(E) = D_1(E) + D_2(E) = G^-(E) - G^+(E). \tag{5}$$

Here $P_1 = \sum_1 |1\rangle\langle 1|$ and $P_2 = \sum_2 |2\rangle\langle 2|$, where indices 1 and 2 run over all atoms to the left and to the right, respectively, of an arbitrary open surface through the electrode-junction-electrode system [9, 22]. P_1 and P_2 satisfy $P_1 + P_2 = \mathbf{1}$, where $\mathbf{1}$ is the identity operator within the Hilbert space spanned by the orthogonal positional basis $\{|n\rangle\}$. $G^{\pm}(E)$ are given by $G^{\pm}(E) = G(E \pm \mathrm{i}\epsilon)$, where ϵ is an infinitesimally small real positive number and $G(z)$ satisfies $(z - H_\mathrm{e})G(z) = G(z)(z - H_\mathrm{e}) = \mathbf{1}$. $G^{\pm}(E)$ are calculated by a standard numerical procedure, described, for instance, in [21, 22].

To define the unperturbed state of the ionic subsystem, we view the ions as a set of independent harmonic oscillators, described by the Hamiltonian

$$H_\mathrm{z} = \sum_{n,\nu} (p_{n\nu}^2/2M_n + M_n\omega_{n\nu}^2 u_{n\nu}^2/2) \tag{6}$$

where $\boldsymbol{p}_n = (p_{nx}, p_{ny}, p_{nz})$ is the momentum of ion n, $\boldsymbol{u}_n = (u_{nx}, u_{ny}, u_{nz})$ is the displacement of the ion from its equilibrium position, and M_n and $\omega_{n\nu}$, with $\nu = x, y, z$, are the mass and the angular frequencies of vibration in each direction, respectively, for the ion. Each ion is placed in a vibrational state, characterized by the quantity

$$N_{n\nu} = \langle a_{n\nu}^\dagger a_{n\nu}\rangle \tag{7}$$

where the angular brackets designate thermal averaging and $a_{n\nu} = (p_{n\nu} - \mathrm{i}M_n\omega_{n\nu}u_{n\nu})/\sqrt{2M_n\hbar\omega_{n\nu}}$ is a bosonic annihilation operator, with $[a_{m\mu}, a_{n\nu}^\dagger] = \delta_{mn}\delta_{\mu\nu}$.

To describe electron–phonon interactions, we view the electrons as independent particles and introduce the electron–oscillator coupling term

$$V_\mathrm{ez} = \sum_{n,\nu} V_{n\nu}u_{n\nu} \tag{8}$$

where

$$V_{n\nu} = \sum_{m\neq n} (|n\rangle\langle m| + |m\rangle\langle n|)\,\partial H_{nm}/\partial R_{n\nu}. \tag{9}$$

Here $\boldsymbol{R}_n = (R_{nx}, R_{ny}, R_{nz})$ is the position of the ion and the derivative in equation (9) is evaluated with the ions at their equilibrium positions.

We now treat V_ez as a perturbation, and use standard lowest-order perturbation theory to calculate the rate of energy transfer, w_n, into ion n in the junction, once the electron–oscillator coupling is turned on [13]. This gives

$$\begin{aligned} w_n = {} & (2\pi\hbar/M_n)\sum_{\alpha,\beta,\nu} (N_{n\nu}+1)\,f_\alpha(1-f_\beta)|\langle\psi_\beta|V_{n\nu}|\psi_\alpha\rangle|^2\delta(E_\beta - E_\alpha + \hbar\omega_{n\nu}) \\ & - (2\pi\hbar/M_n)\sum_{\alpha,\beta,\nu} N_{n\nu}\,f_\alpha(1-f_\beta)|\langle\psi_\beta|V_{n\nu}|\psi_\alpha\rangle|^2\delta(E_\beta - E_\alpha - \hbar\omega_{n\nu}) \end{aligned} \tag{10}$$

Here $|\psi_\alpha\rangle$ and $|\psi_\beta\rangle$ each run over all states $\{|\psi_1\rangle\}$ and $\{|\psi_2\rangle\}$, introduced earlier, and $f_{\alpha,\beta} = f_1(E_{\alpha,\beta})$ if $|\psi_{\alpha,\beta}\rangle$ is one of the right-travelling states $\{|\psi_1\rangle\}$, and $f_{\alpha,\beta} = f_2(E_{\alpha,\beta})$ if $|\psi_{\alpha,\beta}\rangle$ is one of the left-travelling states $\{|\psi_2\rangle\}$. Equation (10) includes a factor of 2 for spin degeneracy. The first term of equation (10) represents processes in which energy is transferred to the ion from the electrons, while the second represents the reverse.

Equation (10) may be obtained directly from the Fermi golden rule. To see this, first we substitute $u_{n\nu} = \mathrm{i}(a_{n\nu} - a_{n\nu}^\dagger)\sqrt{\hbar/2M_n\omega_{n\nu}}$ in equation (8). We may then recognize $(N_{n\nu}+1)(\hbar/2M_n\omega_{n\nu})|\langle\psi_\beta\,|V_{n\nu}|\,\psi_\alpha\rangle|^2$ as the modulus squared of the matrix element for a process, in which an electron is scattered from state $|\psi_\alpha\rangle$ into state $|\psi_\beta\rangle$ and degree of freedom ν of oscillator n gains a quantum of energy, $\hbar\omega_{n\nu}$. Similarly, $N_{n\nu}(\hbar/2M_n\omega_{n\nu})|\langle\psi_\beta\,|V_{n\nu}|\,\psi_\alpha\rangle|^2$ is the modulus squared of the matrix element for a process, in which an electron is scattered from state $|\psi_\alpha\rangle$ into state $|\psi_\beta\rangle$ and degree of freedom ν of oscillator n loses a quantum of

energy, $\hbar\omega_{n\nu}$. Multiplying the transition rate for each process by the respective amount of energy transferred to the ion yields equation (10). The prefactor $f_\alpha(1 - f_\beta)$ accounts for the statistics of the electrons. This prefactor arises naturally if the calculation is carried out in second quantization [13].

The above, lowest-order, perturbative calculation is valid in the limit, assumed in this paper, where the mean time spent by an electron in the nanojunction is smaller than the electron–phonon scattering time in the nanojunction. Equation (10) then describes power dissipation at atomic sites in the nanojunction. To describe power dissipation in the bulk of the adjoining electrodes, one must resort to an appropriate theory of diffusive bulk conduction [14].

Invoking the partial density of states operators $D_1(E)$ and $D_2(E)$, introduced in equation (2), equation (10) may be cast as

$$\begin{aligned} w_n = (2\pi\hbar/M_n) \sum_{i,j=1,2} \int \mathrm{d}E \sum_\nu (N_{n\nu}+1) f_i(E)[1 - f_j(E - \hbar\omega_{n\nu})] \\ \times \mathrm{Tr}[V_{n\nu} D_i(E) V_{n\nu} D_j(E - \hbar\omega_{n\nu})] \\ - (2\pi\hbar/M_n) \sum_{i,j=1,2} \int \mathrm{d}E \sum_\nu N_{n\nu} f_i(E)[1 - f_j(E + \hbar\omega_{n\nu})] \\ \times \mathrm{Tr}[V_{n\nu} D_i(E) V_{n\nu} D_j(E + \hbar\omega_{n\nu})] \end{aligned} \tag{11}$$

where the trace is taken in the positional basis $\{|n\rangle\}$. This result for the local power w_n explicitly takes account of the local electronic structure, as determined by the atomic configuration, via the quantities $V_{n\nu}$ and $D_i(E)$, with $i = 1, 2$. In general, equation (11) must be solved simultaneously and self-consistently with an appropriate model of heat conduction away from the junction, in order to yield the steady-state temperature profile in the junction, in the presence of current flow [13]. In the present paper, however, we wish to study, in a transparent way, the relation between local electronic power dissipation and the local electronic structure. To this end, we simplify equation (11) as follows.

We assume that the electron Green functions, and hence $D_1(E)$ and $D_2(E)$, do not vary significantly over the energy window for conduction, lying between μ_2 and $\mu_1 = \mu_2 + eW$, and we impose the limits $|eW| \gg k\theta$ and $|eW| \gg \hbar\omega_{n\nu}$. Then equation (11) gives a net power into ion n of

$$w_n = -(2\pi\hbar/M_n) \sum_\nu E_{n\nu}(T_{11}^{n\nu} + 2T_{12}^{n\nu} + T_{22}^{n\nu}) + (2\pi\hbar/M_n) \sum_\nu (|eW| - \hbar\omega_{n\nu}) T_{12}^{n\nu} \tag{12}$$

where $E_{n\nu} = N_{n\nu}\hbar\omega_{n\nu}$ and $T_{ij}^{n\nu} = \mathrm{Tr}[V_{n\nu} D_i V_{n\nu} D_j]$, with D_1 and D_2 evaluated at the Fermi level in the absence of the bias.

We make the following further simplification. In the absence of heat conduction, the steady-state condition $w_n = 0$ enables one to solve equation (12) directly for the effective oscillator temperature of ion n [13]. This sets the thermal energy $E_{n\nu}$ in the centre of the nanojunction equal to something of the order of $|eW|$ [13]. In reality, thermal conduction away from the junction maintains $E_{n\nu}$ at a fraction of this value. Then the second term in equation (12) dominates the first. Neglecting $\hbar\omega_{n\nu}$ in comparison with $|eW|$ in that second term, we may then approximately take

$$w_n = (2\pi\hbar/M_n)|eW| \sum_\nu T_{12}^{n\nu} \tag{13}$$

as the net power source at each site in the junction, which heat conduction has to counterbalance in the steady state.

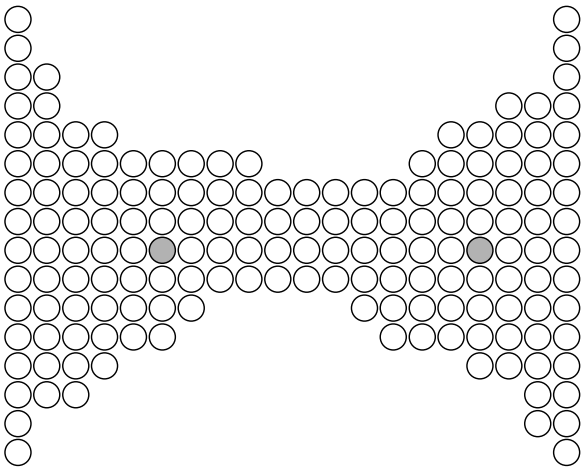

Figure 2. A nanoscale metallic constriction. The details are explained in the text.

3. Results

In all examples in the present paper the electrodes and the junction have a two-dimensional simple square lattice structure. The hopping integrals are taken as $H_{mn} = H_{nm} = -\gamma$, $\gamma > 0$, if m and n are nearest neighbours, and zero otherwise. γ and its derivative with respect to interatomic distance, γ', which enters the local power via equation (9), are parameters of the model. For simplicity, we set $M_n = M$, $\forall n$, where M is a typical atomic mass. The power delivered to site n is calculated from equation (13). The formalism also yields the bond current from site m into site n, to lowest order in W, through the expression [9, 22]

$$I_{mn} = 4(e^2/\hbar)W H_{nm}\,\mathrm{Im}[(D_1)_{mn}] \tag{14}$$

where $(D_1)_{mn} = \langle m|D_1|n\rangle$, with D_1 evaluated at the Fermi level in the absence of the bias. Finally, the local density of states at site n, at zero bias, is given by $D_{nn} = (D_1)_{nn} + (D_2)_{nn}$.

3.1. Nanoscale constriction

We consider the geometry in figure 2. The white circles are metal atoms, with an on-site energy set equal to zero. The two grey circles are impurity atoms with an on-site energy of $+4\gamma$. The electrodes outside the region shown are 20-atom-wide perfect metallic leads, which, in this case, mimic closely enough infinitely wide macroscopic electrodes. The Fermi energy is chosen as $+1\gamma$, close to the centre of the conduction band for a two-dimensional simple square lattice, which extends from -4γ to $+4\gamma$. The zero-voltage elastic conductance [9, 20–22] of the system is $\sigma = 2.8 \times 2e^2/h$. At this Fermi energy there are three open conduction channels in the narrowest, four-atom-wide part of the constriction. The geometry in figure 2, therefore, represents a typical quasiballistic nanoscale metallic constriction, with some surface roughness and with some weak internal disorder.

Figure 3 shows the local power, w_n, calculated from equation (13), and the local current at each atomic site in the constriction, calculated from equation (14). For purposes of presentation, the current arrow plotted at each site is the vector sum of bond currents through that site, divided by two, to reflect the fact that each bond current is shared by two sites. The plot shows that, to a good approximation, in this quasiballistic system the local power is proportional to the local current density. The standard deviation of the ratio of the two, over all sites in figure 2, is about

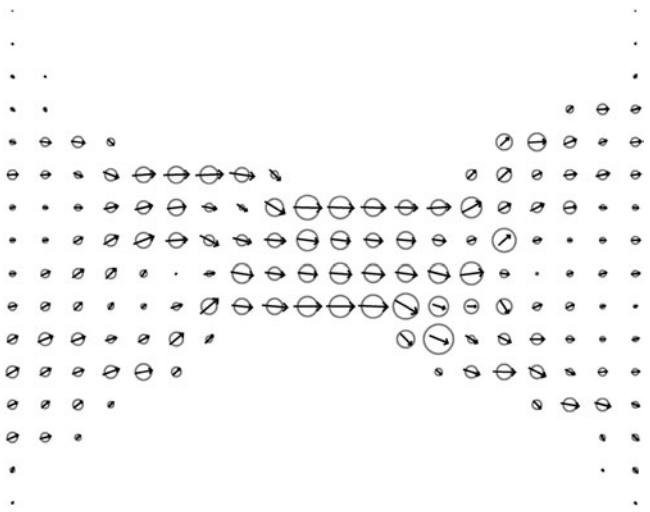

Figure 3. The local power (circles) and the local current (arrows) at each atomic site in the nanoconstriction from figure 2. The local power is proportional to the radius of the circle. The largest circle on the plot represents a power of $0.13 \times (2\pi\hbar/M)|eW|(\gamma'/\gamma)^2$, where M is the atomic mass, W is the applied voltage, and γ and γ' are the nearest-neighbour hopping integral and its derivative with respect to interatomic distance, respectively. The local current is proportional to the length of the arrow. The largest arrow on the plot represents a current of $0.86 \times 2e^2W/h$.

1/4 of the mean value of this ratio. This approximate proportionality between local power and local current was one of the working assumptions in [13]. The constant of proportionality will depend on the material and on the dimensionality of the structure. However, even without knowledge of the precise value of this constant, the spatial relationship between local power and local current in quasiballistic nanostructures—in the regime of validity of equation (13), specified earlier—allows one to make straightforward guesses about the spatial distribution of the dissipated power in such geometries [13].

We have found that this simple relationship rapidly disappears with increasing disorder. For example, in compositionally disordered nanowires with a length exceeding the elastic electron mean free path by a factor of two to three, the proportionality between the local power and the local current is almost completely gone. Instead, large spatial fluctuations develop in the ratio of these two local quantities.

The sum of w_n over all atomic sites in figure 2 comes to $w_{\text{junction}} = 7.3 \times (2\pi\hbar/M)|eW|(\gamma'/\gamma)^2$. Let us compare this with the classical result for the total power, dissipated in the circuit as a whole, $w_{\text{total}} = \sigma W^2$. As stated earlier, the validity of equation (13) requires $|eW| > \hbar\omega$, where $\omega \sim 2\pi \times 5 \times 10^{12}$ Hz is a typical atomic vibration angular frequency. Taking $|eW| = \hbar\omega$, $M \sim 10^{-25}$ kg and $|\gamma/\gamma'| \sim 10^{-10}$ m thus gives an upper bound—within the range of validity of the calculation—on $w_{\text{junction}}/w_{\text{total}}$ of order 1/10. There is, therefore, no contradiction between the basic notion in our model that the highest power dissipation per atom occurs in the nanojunction, and the expectation that most of the global power is dissipated in the rest of the system [14].

Let us test one more aspect of our model against the numerical results. Let us consider the mean electron lifetime, τ_e, between inelastic electron–phonon collisions in the junction. Both processes, represented by the two terms in equation (10), limit this lifetime. Without detailed calculation [13], appealing to the Fermi golden rule, as an order-of-magnitude estimate of τ_e

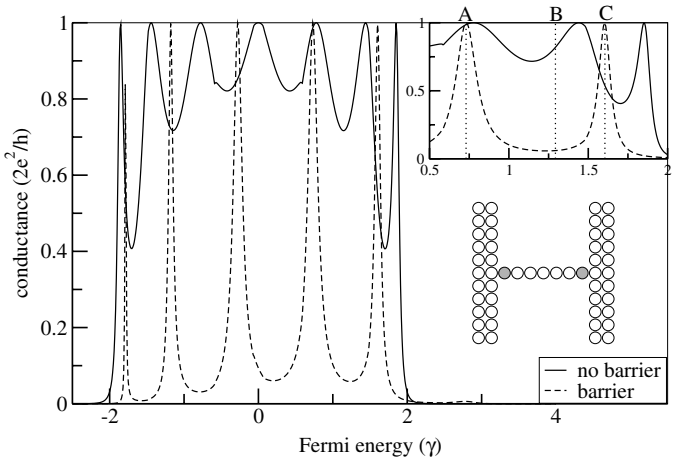

Figure 4. Conductance as a function of Fermi energy for an atomic chain between two metallic electrodes. The geometry is shown in the inset. The solid curve gives the conductance for the case where all atoms are the same. The broken curve gives the conductance for the case where the two end atoms in the chain are weak scatterers, creating a double barrier for electrons. The details are discussed in the text.

in the vicinity of site n, we may take

$$1/\tau_e \sim (\gamma/Mf)(\gamma'/\gamma)^2(\gamma D_{nn})(2N+1) \tag{15}$$

where $f \sim 5 \times 10^{12}$ Hz is a typical atomic vibration frequency and N is a typical number of vibrational quanta per degree of freedom, per atom. The local density of states, D_{nn}, in the present structure is around $0.16\,\gamma^{-1}$. $(2N+1)$ does not exceed something of order 10 over the temperature range from 0 K up to a typical metal melting temperature. Then, with $\gamma \sim 2$ eV, we find a lower bound on τ_e of the order of 10^{-14} s. This corresponds to an inelastic electron mean free path of at least 10 nm, or tens of atoms, exceeding the length of the nanojunction. Therefore, we have not violated the range of validity of the perturbative calculation of the local power in the junction.

An estimate of the actual steady-state temperature in a biased metallic nanojunction, based on the assumption of diffusive lattice heat conduction limited by phonon–electron scattering, is given in [13]. The resultant local temperature rise leads to a situation where the nanojunction is hot, as far as atoms are concerned, but is still ballistic, as far as electrons are concerned, inasmuch as—as shown above—any electron experiences, on average, little inelastic scattering while crossing the junction [13]. The local heating in this regime, therefore, need not be accompanied by a significant change in the conductance of the system.

3.2. Atomic chain

The next example is a seven-atom-long atomic chain between two 11-atom-wide semi-infinite perfect leads, as shown in the inset in figure 4. We consider two cases. In the first case, all atoms have the same on-site energy, set equal to zero. In the second case, the on-site energy on the two end atoms in the chain, shown by the grey circles in the inset in figure 4, is set equal to $+2\gamma$. These atoms may then be taken to represent impurities, or another relatively weak scatterer, creating a double barrier for electrons incident from the electrodes.

The zero-voltage elastic conductance, as a function of Fermi energy, for these two cases is shown in figure 4. In the case without the barrier atoms, the conductance stays close to

	Fermi energy	maximum current	maximum power	maximum density of states
A	0.730	0.986	0.130	0.288
B	1.293	0.820	0.099	0.288
C	1.605	0.538	0.060	0.271

Figure 5. The local power (upper semicircles), the local current (arrows), and the local density of states (lower semicircles) at the energies marked A, B, and C in figure 4, for the case without the double barrier. Power is in units of $(2\pi\hbar/M)|eW|(\gamma'/\gamma)^2$, where M is atomic mass, W is the applied voltage, and γ and γ' are the nearest-neighbour hopping integral and its derivative with respect to interatomic distance, respectively. The density of states is in units of γ^{-1}. Current is in units of $2e^2W/h$. The local power and density of states are proportional to the radius of the respective semicircle, and the current is proportional to the length of the arrow.

the quantum unit of $2e^2/h$ over the entire conduction band for a one-dimensional chain. The waviness in the conductance curve is due to multiple reflections from the two chain–electrode contacts [24]. In the case with the double barrier, this waviness evolves into sharp conductance peaks, separated by deep troughs. The peaks correspond to resonant transmission through quasibound states in the region between the barriers [22].

We now calculate the local power, local current, and local density of states at the energies marked A, B, and C in figure 4. The results for the case without the barrier, shown in figure 5, are similar to those for the nanoconstriction from figure 2. The results for the case with the double barrier, shown in figure 6, exhibit qualitatively different behaviour. At the conductance resonances A and C, we see a huge enhancement in the local power at particular atoms in the chain. For example, at energy A the conductance, and the maximum local current, is essentially the same in the cases without and with the double barrier, while the maximum local power within the chain increases by an order of magnitude in going from the first to the second case.

The origin of this enhancement is evident from the corresponding enhancement in the local density of states at resonance. Physically, at resonance, passing electrons become temporarily

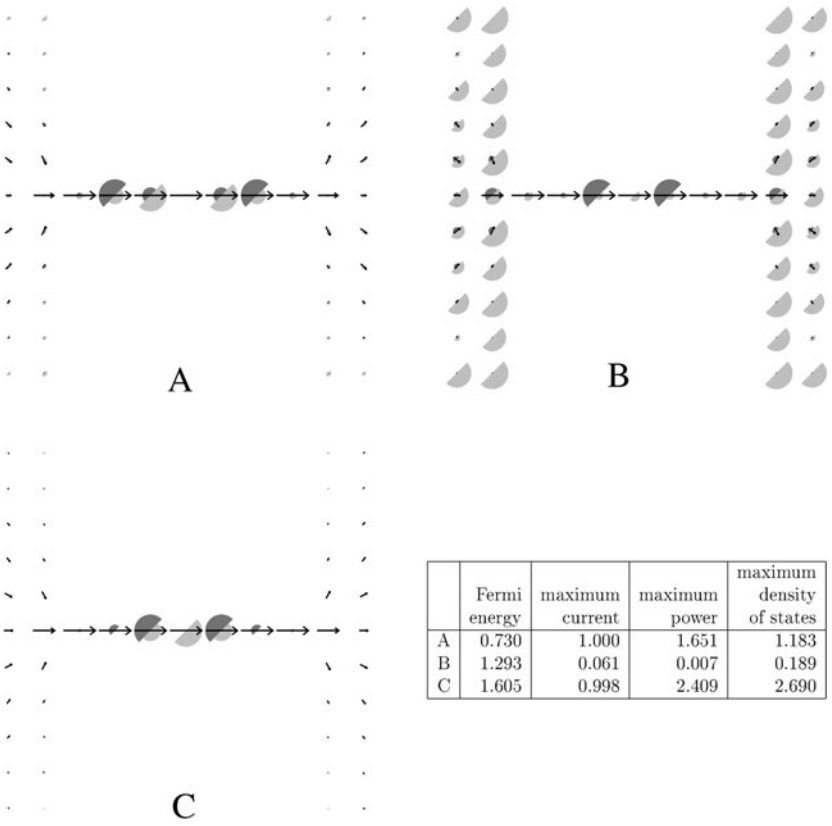

	Fermi energy	maximum current	maximum power	maximum density of states
A	0.730	1.000	1.651	1.183
B	1.293	0.061	0.007	0.189
C	1.605	0.998	2.409	2.690

Figure 6. The same as figure 5, but for the case with the double barrier in the atomic-chain geometry of figure 4.

trapped in the quasibound state that gives rise to the resonance. They 'buzz around' in the region inside the double barrier for an enhanced period of time, giving them an enhanced opportunity to interact with, and dissipate energy at, the vibrating ions in that region. The precise spatial distribution of the local power and density of states at resonance is related to the spatial wavefunction of the corresponding quasibound state [22].

To test the validity of our model, we may use equation (15) to obtain a lower bound on the inelastic electron lifetime at resonance of the order of 10^{-15} s. This lower bound is of the same order of magnitude as the electron residence time in the respective quasibound state, which may be estimated from the energy width of the resonances in figure 4. The electron residence time thus does not exceed the inelastic electron lifetime, as is required for the validity of our model.

Equation (13) was derived in the linear regime, where electronic properties do not vary significantly over the energy window for conduction. In the present case this requires $|eW|$ to be less than something of the order of the width of a conductance resonance, or $0.2\gamma \sim 0.4$ eV. At larger voltages, we must revert to equation (11) and perform the energy integrations therein fully.

With $W = 0.1$ V, or a few $\hbar\omega$, with the earlier representative values for the other quantities in equation (13), at resonance the maximum power per atom in the chain is of the order of one $\hbar\omega$ per thermal vibration period. The resultant steady-state temperature in the chain depends on the mechanism of thermal conduction away from the junction [13]. Even if heat is carried away

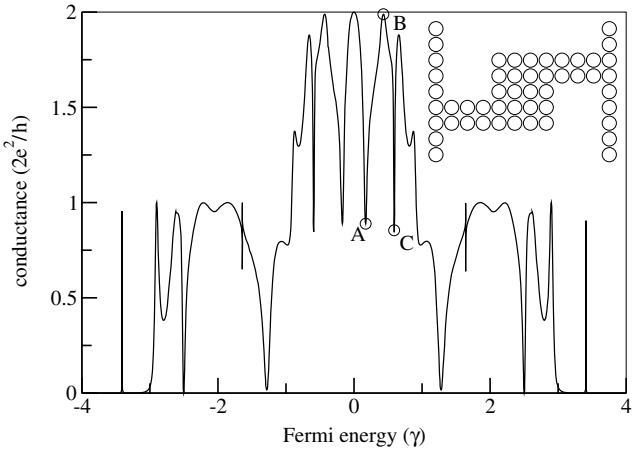

Figure 7. Conductance as a function of Fermi energy for a nanowire with an S-shaped bend between two metallic electrodes. The geometry is shown in the inset.

by ballistic one-dimensional phonons, without any scattering, at zero ambient temperature, to balance this power injection in the system at resonance, the thermal energy density in the chain must be of the order of $\hbar\omega$ per atom. This corresponds to an effective local temperature of 100–200 K.

3.3. Irregular nanowire

The geometry for the last example is shown in the inset in figure 7. It is a defect-free nanowire with an S-shaped bend, attached to wide perfect electrodes. Figure 7 shows the conductance for this system as a function of Fermi energy. The maximum value of the conductance, $2 \times 2e^2/h$, is limited by the width—two atoms—of the narrow entrance and exit branches of the nanowire. The conductance curve exhibits sharp minima. To see their origin, we have calculated the local power, local current, and local density of states at the energies marked A, B, and C in figure 7. The results are displayed in figure 8.

Point B shows similar behaviour to the quasiballistic constriction from figure 2. At points A and C we see a great enhancement in the local power, accompanied by an enhancement in the local density of states, at atoms in the top left and bottom right corners of the central island in the nanowire. The actual local current in those sheltered regions is very small compared with the mainstream regions. Close inspection of the results for point A shows that current flow in the sheltered corners is vortical.

Physically, the behaviour seen at energies A and C is analogous to what we found for the atomic chain with the double barrier. The enhancement in the local density of states and in the local power is due to the formation of quasibound states—at special energies—in the sheltered corners of the central island. Electrons at those energies spend enhanced periods of time in these corners, resulting in enhanced energy exchange with the oscillators therein. The only qualitative difference from the case of the double barrier is that at resonance in the double barrier the respective quasibound state acts as a stepping stone for incident electrons and results in a conductance peak, whereas in the present case, the formation of quasibound electron ‘traps’ at the corners results in a reduction in overall transmission.

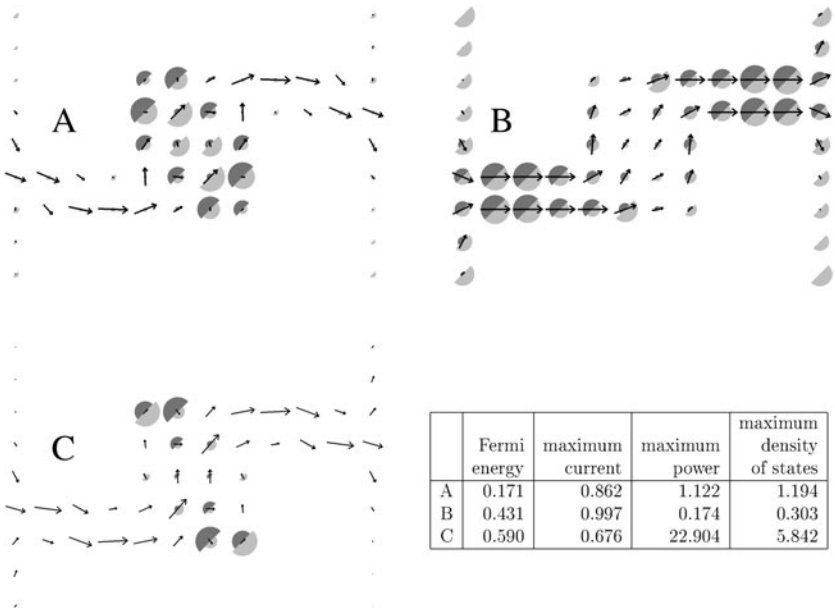

	Fermi energy	maximum current	maximum power	maximum density of states
A	0.171	0.862	1.122	1.194
B	0.431	0.997	0.174	0.303
C	0.590	0.676	22.904	5.842

Figure 8. The local power (upper semicircles), the local current (arrows), and the local density of states (lower semicircles) at the energies marked A, B, and C in figure 7. The units are the same as in figure 5.

4. Summary

The particular electronic model used in this paper was deliberately chosen in a simple way in order to enable us to extract the following qualitative conclusions. First, it is possible to have large local power dissipation in a nanoscale junction, even when the time spent by individual electrons in the junction is much less than the inelastic electron lifetime. There is no contradiction between this statement and the expectation that most of the total power, dissipated in the circuit as a whole, should be deposited in the electrodes.

Second, in simple quasiballistic geometries—in the voltage range where equation (13) is valid—the power per atom locally is proportional to the local current density. This spatial relation between the two quantities allows simple guesses of the spatial distribution of the dissipated power in such geometries.

Third, there can be greatly enhanced power dissipation at special atoms in cases of resonant and anti-resonant transmission. This enhancement occurs, because at resonance or anti-resonance electrons get temporarily trapped in quasibound states, allowing extra time for electron–phonon interactions locally. An example of an anti-resonant system is the bent nanowire in figure 7. Examples of resonant systems are the double-barrier formation in figure 4 and molecular junctions between two metallic electrodes [8,25]. The enhanced power dissipation in such systems increases their susceptibility to current-induced modifications.

The actual steady-state temperature profile in a biased nanojunction depends on the mechanism of thermal conduction away from the junction. The estimate given above in connection with the resonant double barrier, as well as the earlier estimates in [5,13], indicate a significant local temperature rise in metallic nanojunctions even at modest voltages. To obtain a more accurate picture of the steady-state temperature profile in a nanoconductor, ultimately one must solve equation (11) simultaneously with an appropriate atomistic model of thermal conduction away from the junction. This work is currently in progress.

Acknowledgment

TNT is grateful to EPSRC for support.

References

[1] Lang N D 1992 *Phys. Rev.* B **45** 13 599
[2] Lang N D 1994 *Phys. Rev.* B **49** 2067
[3] Todorov T N, Hoekstra J and Sutton A P 2000 *Phil. Mag.* B **80** 421
[4] Di Ventra M and Pantelides S T 2000 *Phys. Rev.* B **61** 16 207
[5] Todorov T N, Hoekstra J and Sutton A P 2001 *Phys. Rev. Lett.* **86** 3606
[6] Mingo N, Yang L and Han J 2001 *J. Phys. Chem.* B **105** 11 142
[7] Todorov T N 2001 *J. Phys.: Condens. Matter* **13** 10 125
[8] Di Ventra M, Pantelides S T and Lang N D 2002 *Phys. Rev. Lett.* **88** 046801
[9] Todorov T N 2002 *J. Phys.: Condens. Matter* **14** 3049
[10] Ralls K S, Ralph D C and Buhrman R A 1989 *Phys. Rev.* B **40** 11 561
[11] Holweg P A M, Caro J, Verbruggen A H and Radelaar S 1992 *Phys. Rev.* B **45** 9311
[12] Chen Z and Sorbello R S 1993 *Phys. Rev.* B **47** 13 527
[13] Todorov T N 1998 *Phil. Mag.* B **77** 965
[14] Gurevich V L 1997 *Phys. Rev.* B **55** 4522
[15] Muller C J, van Ruitenbeek J M and de Jongh J L 1992 *Phys. Rev. Lett.* **69** 140
[16] van den Brom H E, Yanson A I and van Ruitenbeek J M 1998 *Physica* B **252** 69
[17] van den Brom H E 2000 Noise properties of atomic-size contacts *Doctoral Thesis* University of Leiden
[18] Walkup R E, Newns D M and Avouris Ph 1993 *Phys. Rev.* B **48** 1858
[19] Eigler D M, Lutz C P and Rudge W E 1991 *Nature* **352** 600
[20] Todorov T N, Briggs G A D and Sutton A P 1993 *J. Phys.: Condens. Matter* **5** 2389
[21] Todorov T N 1996 *Phys. Rev.* B **54** 5801
[22] Todorov T N 1999 *Phil. Mag.* B **79** 1577
[23] Sutton A P, Todorov T N, Cawkwell M J and Hoekstra J 2001 *Phil. Mag.* B **81** 1833
[24] Todorov T N and Briggs G A D 1994 *J. Phys.: Condens. Matter* **6** 2559
[25] Lang N D and Avouris Ph 2001 *Phys. Rev.* B **64** 125323